Nicotine Enhancement of Fast Excitatory Synaptic Transmission in CNS by Presynaptic Receptors

Daniel S. McGehee, Mark J. S. Heath, Shari Gelber, Piroska Devay, Lorna W. Role*

The behavioral and cognitive effects of nicotine suggest that nicotinic acetylcholine receptors (nAChRs) participate in central nervous system (CNS) function. Although nAChR subunit messenger RNA (mRNA) and nicotine binding sites are common in the brain, there is little evidence for synapses mediated by nAChRs in the CNS. To test whether CNS nAChRs might modify rather than mediate transmission, the regulation of excitatory synaptic transmission by these receptors was examined. Nanomolar concentrations of nicotine enhanced both glutamatergic and cholinergic synaptic transmission by activation of presynaptic nAChRs that increased presynaptic $[Ca^{2+}]_i$. Pharmacological and subunit deletion experiments reveal that these presynaptic nAChRs include the $\alpha 7$ subunit. These findings reveal that CNS nAChRs enhance fast excitatory transmission, providing a likely mechanism for the complex behavioral effects of nicotine.

The complex and potent psychophysical effects of nicotine suggest that nAChRs may be important in alterations of short-term memory, attention, and anxiety (*1*). Likewise, the disruption of cholinergic systems in diseases such as Alzheimer's causes impairment of cognition. Despite this evidence for a prominent role of nAChRs in CNS function, electrophysiological studies of candidate cholinergic synapses in the CNS have failed to demonstrate nAChR-mediated synaptic transmission (*2*, but see *3*). Even at synapses with presynaptic choline acetyltransferase expression and postsynaptic nAChRs, synaptic transmission is mediated by transmitters other than ACh (*4*, *5*). In addition, the serum concentrations of nicotine achieved during cigarette smoking are far lower than those required for activation of CNS nicotinic receptors (*6*). Thus, the role of CNS nAChRs and the site of nicotine action remain unknown.

To address this problem we examined the effects of low concentrations of nicotine on fast glutamatergic synaptic transmission in CNS neurons and compared the effects seen there with those induced by nicotine at a peripheral cholinergic synapse. We found that presynaptic nAChRs are distinct in pharmacology and subunit composition from somatic nAChRs and potently enhance both types of fast excitatory synaptic transmission.

Nicotine effects at excitatory synapses. The effect of nicotine on transmission was first tested at the excitatory synapse between neurons of the medial habenula nucleus (MHN) and the interpeduncular nucleus (IPN), a central limbic relay thought to be involved in arousal and attentive behavior (*7*). Although both MHN and IPN neurons express nAChRs (*8*, *9*) and many MHN neurons express choline acetyltransferase (*9*, *10*), previous in vivo studies suggested that transmission is mediated by an excitatory amino acid (*5*). Our initial characterization of the transmission at synapses between MHN and IPN neurons in vitro confirmed these findings and demonstrated that the proposed excitatory transmitter is glutamate: Synaptic activity was blocked by 6-cyano-7-nitroquinoxaline-2,3-dione (CNQX, 50 μM) (Figs. 1A and 2B) indicating that non–*N*-methyl-D-aspartic acid–type glutamate receptors mediate transmission. The ability of nicotine to modify glutamatergic transmission was assessed by recording from IPN neurons with concurrent extracellular stimulation of neighboring microexplants including the MHN (*11*) (Fig. 1). Application of nicotine (100 nM) to sites of MHN-IPN contact enhanced glutamatergic transmission: The amplitude of the evoked currents more than doubled and the number of failures in response to a constant applied stimulus was decreased (Fig. 1).

Enhancement of evoked synaptic transmission by nicotine could be due to alterations in either pre- or postsynaptic function, or both. To examine the locus of nicotine-induced enhancement we analyzed spontaneous excitatory postsynaptic currents (sEPSC) (*11*). In the presence of tetrodotoxin (TTX, 2 μM), to block suprathreshold activity, the frequency of spontaneous synaptic currents was low (<1/s, on average). Application of nicotine (30 nM to 10 μM) increased sEPSC frequency without detectable alteration of postsynaptic holding current in 42 percent of the cells tested (Fig. 2, A to D) (*12*). The increase in sEPSC frequency persisted for 20 to 40 s on average, declining toward control event frequency in the continued presence of nicotine for most cells. However, in 40 percent of the responsive synapses, enhanced release persisted for as much as 5 to 6 min in the continued presence of nicotine (Fig. 2B) with desensitization apparent with high concentrations of nicotine (as in Fig. 2D). Analysis of the amplitudes of the spontaneous synaptic currents indicates that nicotine increased sEPSC frequency without altering the size of these currents (Fig. 2C). Thus, nicotine-induced enhancement of glutamatergic transmission involved alteration in presynaptic function, that is, increased probability of release, rather than a postsynaptic effect, such as a change in sensitivity of the postsynaptic neuron to transmitter. The half-maximal effective concentration (EC_{50}) for the enhancement of glutamate release at MHN-IPN synapses is ~120 nM nicotine (Fig. 2D), consistent with activation of a receptor of sufficiently high affinity to be gated by nicotine at concentrations equivalent to

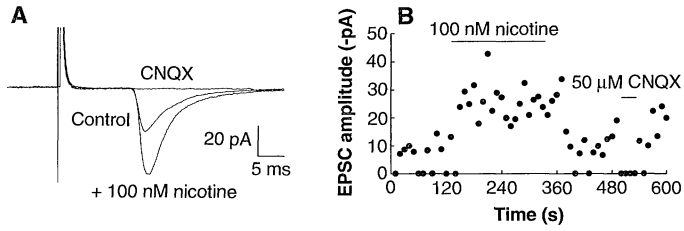

Fig. 1. Evoked synaptic transmission at MHN-IPN synapses mediated by glutamate was enhanced by nicotine. (**A**) Averages of 20 evoked synaptic currents (EPSCs) under control conditions, with application of nicotine (100 nM) or CNQX (50 μM). EPSCs were stimulated by use of an extracellular bipolar electrode placed in the MHN explant (0.1 Hz). Evoked responses in an innervated IPN neuron were recorded with the perforated patch technique. (**B**) Evoked synaptic currents in an innervated IPN neuron before, during, and after application of nicotine. Comparable enhancement of EPSC amplitude by nicotine was seen at four of nine synaptic pairs tested.

D. S. McGehee, S. Gelber, P. Devay, and L. W. Role are in the Department of Cell Biology and Anatomy in the Center for Neurobiology and Behavior, Columbia University, College of Physicians and Surgeons, 722 West 168th Street, P. I. Annex, New York, NY 10032, USA. M. J. S. Heath is in the Department of Anesthesiology, Columbia University, College of Physicians and Surgeons, 722 West 168th Street, P. I. Annex, New York, NY 10032, USA.

*To whom correspondence should be addressed.

those in the serum of a moderate smoker [10 to 100 nM (6)]. The cholinergic fibers that project in the fasciculus retroflexus to the IPN (*10*) provide a local source of endogenous agonist for the enhancement of glutamatergic transmission.

The observed enhancement of both spontaneous and evoked glutamate transmission by a second fast excitatory transmitter (for example, ACh) allows for rapid and dramatic modification of signaling between neurons. To test whether nicotine might similarly regulate synapses where transmission is mediated by a fast excitatory transmitter other than glutamate, we examined cholinergic synaptic transmission at synapses between neurons of the visceral motor nucleus of Terni (VMT) and the lumbar sympathetic ganglion (LSG) (*13*). Transmission between VMT and LSG neurons was blocked completely with neuronal nAChR antagonists including hexamethonium, mecamylamine, d-tubocurarine, or neuronal bungarotoxin (nBgTx), consistent with postsynaptic nAChRs mediating transmission (*14*). Nicotine enhanced sEPSC frequency in this preparation, in the presence of TTX (2 μM) (Fig. 2, E to G), without significant changes in amplitude (Fig. 2G). Nicotine induced synaptic enhancement at most VMT-LSG synapses (78 percent, n = 45), in contrast to the more confined effects of nicotine at MHN-IPN synapses (42 percent, n = 33). At VMT-LSG synapses nicotine enhanced transmission at concentrations nearly two orders of magnitude lower than those that evoke detectable macroscopic nAChR-mediated currents in the LSG neurons (Fig. 2H). More detailed pharmacological assessment of the presynaptic effect of nicotine was precluded due to the presence of postsynaptic nAChRs gated by nicotine concentrations ≥ 3 μM. The difference in agonist sensitivity of the pre- and postsynaptic effects of nicotine may reflect distinct binding affinities of the nAChRs involved. This interpretation is complicated, however, by the inherently indirect nature of the physiological assay employed.

Nicotinic AChR localization and the role of Ca^{2+}. Although the most parsimonious explanation for presynaptic enhancement by nicotine is a direct activation of nAChRs localized on the presynaptic MHN and VMT terminals, we tested the possible contribution of postsynaptic nAChRs linked to the generation of a retrograde messenger (*15*). In view of the relatively high permeability of neuronal nAChRs to Ca^{2+} (*16*) as well as the Ca^{2+}-dependent synthesis of candidate retrograde messengers known to be active in vertebrate neurons, we tested whether direct manipulations of postsynaptic intracellular Ca^{2+} concentration, $[Ca^{2+}]_i$, could alter nicotine-induced synaptic enhancement (*17*). Elevation of $[Ca^{2+}]_i$ by imposed depolarization of the postsynaptic neuron (3 s, 10 Hz, −80 mV to 0 mV, 50 ms duration) did not change the frequency or amplitude of recorded sEPSCs. Subsequent application of nicotine enhanced synaptic transmission equivalent to control (Fig. 3A). Likewise, buffering of postsynaptic $[Ca^{2+}]_i$ to ~10^{-8} M by internal perfusion with 10 mM BAPTA had no effect on either spontaneous synaptic activity or synaptic enhancement by nicotine (Fig. 3C). These results are consistent with a direct presynaptic action of nicotine in the enhancement of both glutamatergic and cholinergic transmission rather than an indirect mechanism involving a Ca^{2+}-dependent retrograde messenger. These experiments were designed to test the involvement of a known retrograde messenger, and as such, did not allow us to rule out contribution of as yet unidentified Ca^{2+}-independent signaling pathways. Additional evidence that syn-

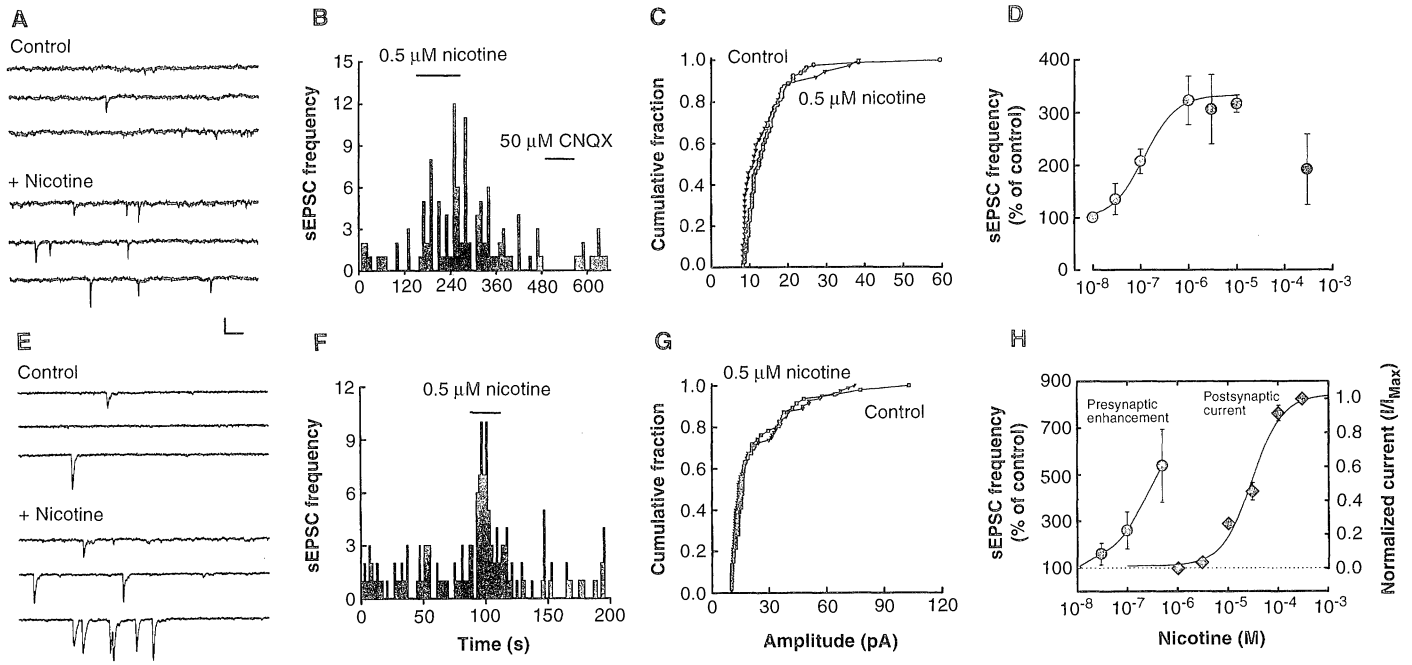

Fig. 2. Enhancement of spontaneous synaptic transmission by nicotine at both glutamatergic and cholinergic synapses. Representative recordings of spontaneous synaptic currents at an MHN-IPN synapse (**A** to **D**) and a VMT-LSG synapse (**E** to **H**) (2 μM TTX present throughout the recordings). Frequency histogram of sEPSC activity in an innervated IPN neuron (B) and an innervated LSG neuron (F) under control conditions and in the presence of nicotine (500 nM) or CNQX (50 μM) as indicated (bin sizes are 10 and 2 s in B and F, respectively). Cumulative distributions of sEPSC amplitudes from an IPN neuron (C) and an LSG neuron (G) during control recording and in the presence of nicotine (500 nM): Increased sEPSC frequency occurred without alteration of sEPSC amplitude. (D) Concentration dependence of nicotine-induced enhancement of MHN-IPN synapses (EC_{50} = 170 nM, n = 4 at each concentration). The response to 300 μM was not used in the curve-fitting as the increase in sEPSC frequency was attenuated due to rapid desensitization at this high concentration. (H) Concentration dependence of nicotine-induced increases in sEPSC frequency plotted with nicotine-evoked macroscopic currents in innervated LSG neurons. The threshold for presynaptic enhancement occurred at concentrations of nicotine two orders of magnitude lower than required for activation of postsynaptic macroscopic current responses (postsynaptic n = 5; presynaptic n = 4, 5, 15, and 4 for 30, 100, 500, and 1000 nM, respectively. Calibration: (A and E) 10 pA, 50 m.

aptic enhancement by nicotine is independent of postsynaptic-derived factors was provided by Ca^{2+}-imaging studies.

Although changes in postsynaptic $[Ca^{2+}]_i$ were not involved in nicotine-induced synaptic enhancement, Ca^{2+} influx by activation of presynaptic nAChRs appeared to be essential. Assay of sEPSC frequency with concurrent superfusion of nominally Ca^{2+}-free solution (no Ca^{2+} added) revealed that application of nicotine (0.1 to 1 μM) was now without effect (Fig. 3F). In addition, increasing the external Ca^{2+} concentration ($[Ca^{2+}]_e$) directly influenced the nicotine-induced enhancement of sEPSC frequency. On average, nicotine (100 nM) enhanced sEPSC frequency to 161 ± 12 percent of control with 1.0 mM $[Ca^{2+}]_e$ ($n = 8$). When $[Ca^{2+}]_e$ was increased to 2.0 mM, the (100 nM) enhancement by nicotine was 213 ± 10 percent of control ($n = 4$).

In view of the dependence of this response on $[Ca^{2+}]_e$ and the known permeability of neuronal nAChRs to Ca^{2+}, we next tested whether nAChRs on presynaptic neurites induced Ca^{2+} influx, independent of the presence of postsynaptic neurons. Presynaptic microexplants were maintained in vitro in the absence of postsynaptic neurons and, after 2 days in culture when process outgrowth was extensive, were loaded with the Ca^{2+} indicator dye, fura-2. Fluorescence imaging of intracellular $[Ca^{2+}]$ in presynaptic neurites revealed robust and reversible increases in $[Ca^{2+}]_i$ after nicotine application (Fig. 3G) (*18*). The nicotine-induced increase in $[Ca^{2+}]_i$ was seen throughout the neurites, including the most distal extensions, and was not dependent upon action potential propagation (Figs. 3G and 4B). The data of Figs. 2 and 3 indicate that (i) the effect of nicotine on synaptic activity was dependent upon $[Ca^{2+}]_e$, (ii) manipulations of intracellular postsynaptic $[Ca^{2+}]$ did not influence nicotine responses, (iii) nicotine enhancement of transmission had a lower EC_{50} than that of activation of postsynaptic nAChRs on LSG neurons, (iv) nicotine facilitated transmission without altering sEPSC amplitude, and (v) nicotine activated increases in $[Ca^{2+}]_i$ in neurites of presynaptic cells in the absence of target neurons. Thus, nicotine-enhanced synaptic transmission through the activation of nAChRs localized to presynaptic structures and independent of retrograde signals that might be generated by the postsynaptic neurons.

Characterization of presynaptic nAChRs. The identification of presynaptic nAChRs that enhance both glutamate and ACh transmission provides a likely site of action for both endogenous and exogenous cholinergic agents in the CNS. It is thus essential to define the physiological and pharmacological profile of these presynaptic nAChRs. The subunit composition of nAChRs affects their physiological and pharmacological profiles, which are dependent on the particular α and β subunits expressed in heterologous systems (*19*). Specifically, heterologous expression of the α7 subunit yields channels that have high permeability to Ca^{2+} (Ca^{2+}/Na^{+} ratio ~20:1) (*20*) and in their susceptibility to block by α-bungarotoxin (αBgTx) (*21*). We know from polymerase chain reaction analysis of mRNA from dorsal spinal cord, that α7, along with nAChR subunits α2, α3, α4, α5, α8, β2, and β4 are expressed in the region that includes the preganglionic nucleus (*22*). In light of these observations, we examined the effects of αBgTx pretreatment (100 nM) on nicotine-induced synaptic enhancement and presynaptic Ca^{2+}-influx.

Treatment with αBgTx blocked the nicotine-induced enhancement of evoked synaptic activity at MHN-IPN synapses (Fig. 4A). The nicotine-induced increase in $[Ca^{2+}]_i$ was also inhibited by αBgTx (500 nM; Fig. 4B). Enhancement of sEPSC frequency by nicotine at both MHN-IPN and

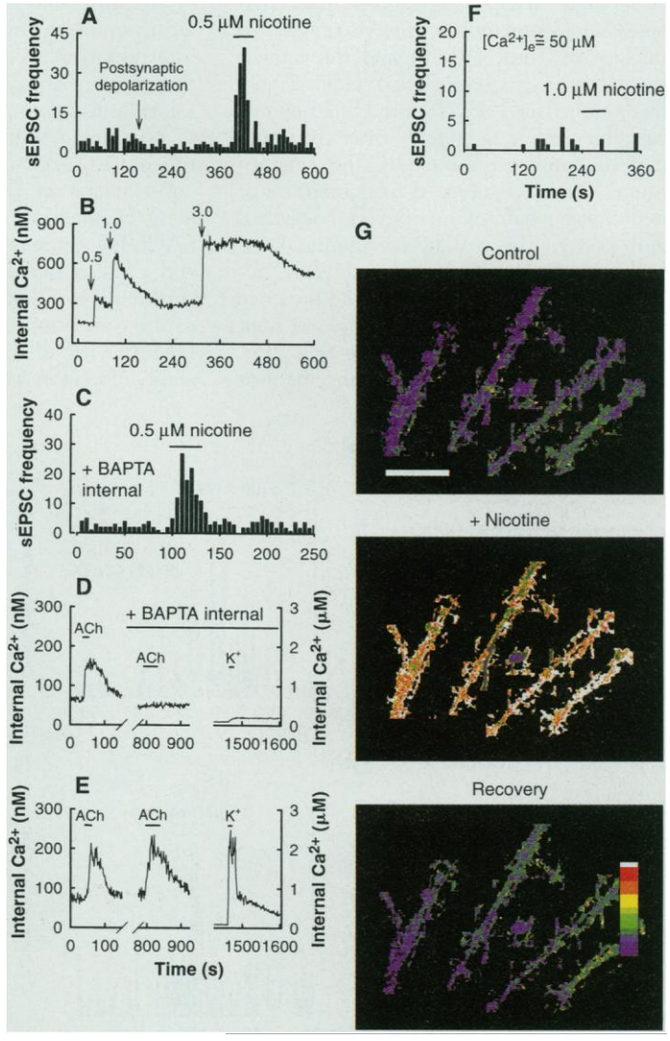

Fig. 3. Effect of postsynaptic $[Ca^{2+}]_i$ and Ca^{2+} influx into presynaptic neurites on nicotine-induced synaptic enhancement. (**A**) Increases in postsynaptic $[Ca^{2+}]_i$ by direct depolarization of innervated LSG neurons did not effect nicotine-induced synaptic enhancement (V_h = −80 mV, voltage step to 0 mV, 50 ms, 20 Hz, 3 s; nicotine, 0.5 μM). (**B**) Depolarizing voltage steps induced increases in $[Ca^{2+}]_i$. In simultaneous Ca^{2+}-imaging and patch-clamp recording, the voltage step protocol described in (A) was applied for 0.5, 1.0, and 3.0 s at the designated time points. The patch electrode used to apply the voltage steps to this cell contained fura 2 pentapotassium salt (200 μM) without EGTA or BAPTA. (**C**) Reduction of postsynaptic $[Ca^{2+}]_i$ by dialysis with BAPTA (10 mM) neither reduced nor increased nicotine- induced synaptic enhancement. (**D**) The effects of internal dialysis with BAPTA (10 mM) on $[Ca^{2+}]_i$. ACh (50 μM) induced an increase in $[Ca^{2+}]_i$ in a sympathetic neuron loaded with fura 2-AM (*18*). A gigaseal was then formed on this cell using a patch electrode filled with internal solution including BAPTA (10 mM) and fura 2 pentapotassium salt (200 μM). Whole-cell access was maintained throughout the remainder of the $[Ca^{2+}]_i$ measurements and no holding current was applied to the cell (current clamp recording mode). A second application of ACh (50 μM, 30 s) did not induce an increase in $[Ca^{2+}]_i$. To test the ability of the BAPTA to buffer Ca^{2+} entering through voltage-gated channels, external solution containing KCl (60 mM) was applied for 30 s (right hand trace). The right hand axis applies to the right hand trace only. (**E**) A neighboring cell responded to ACh application and to the high KCl concentration with increases in $[Ca^{2+}]_i$. (**F**) Reduction of external $[Ca^{2+}]$ to ≤50 μM abolishes nicotine-induced synaptic enhancement. For (A), (C), and (F), $n = 3$ in both VMT-LSG and MHN-IPN preparations. (**G**) Nicotine increased $[Ca^{2+}]_i$ in presynaptic neurites in the absence of postsynaptic neurons. Pseudocolor fura-2 images of intracellular $[Ca^{2+}]$ in neurite fascicles emanating from a dorsal spinal cord explant including the VMT. Nicotine (10 μM) increased $[Ca^{2+}]_i$ independent of suprathreshold activity (TTX, 2 μM). One color increment ≈70 nM change in $[Ca^{2+}]_i$, white indicates internal $[Ca^{2+}]$ in excess of 1 μM. Scale bar, 10 μm.

VMT-LSG synapses was also inhibited by αBgTx (Fig. 4C), without alteration of sEPSC amplitude in either preparation. Examination of the concentration dependence of αBgTx revealed a half-maximal inhibitory concentration (IC_{50}) in the range of ~70 nM, in contrast to the IC_{50} of ~1 nM for αBgTx inhibition of α7 homomeric channels (Fig. 4D) (*21*). Thus, the αBgTx-sensitive nAChRs that underlie the nicotinic enhancement of both spontaneous and evoked synaptic transmission are pharmacologically distinct from the postsynaptic nAChRs mediating transmission. In addition, the apparent pharmacological differences between α7 homomers (*21*) and the presynaptic nAChRs suggests, but does not prove, that the latter may comprise a non-homomeric α7-containing complex. Immunoprecipitation data indicate that α7 can combine with α8 to form heteromeric receptors (*23*), and it remains possible that other known classes of nAChR subunits may associate with α7 as well. This complex could also include an as yet unidentified molecular component that contributes to the unique pharmacology.

As a direct test of the participation of α7 subunits in presynaptic nAChR complexes, we first treated VMT-LSG cultures with a 15-base DNA oligonucleotide targeted to the α7 mRNA translation initiation site (*24*). After treatment of the cocultures with antisense and control oligonucleotides for 72 hours, the αBgTx-sensitive component of synaptic enhancement by nicotine was abolished (Fig. 5A). Treatment with a sense oligonucleotide or with oligonucleotides containing three mismatched bases were without effect (*24, 25*). Further verification of antisense-specific decreases in α7 protein was provided by protein immunoblot analysis of extracts from antisense and control oligomer treated cultures: α7 antisense specifically decreased the amount of α7 immunoreactive protein (Fig. 5B) (*26*). Because nicotine application still elicits detectable synaptic enhancement in α7 antisense treated cultures, albeit through αBgTx-insensitive receptors, deletion of α7-containing, αBgTx-sensitive presynaptic receptors may be accompanied by compensatory changes in synthesis or targeting of high-affinity-αBgTx-insensitive nAChRs to presynaptic sites. If the presynaptic nAChRs normally expressed include α7 with other subunit types, the receptors assembled after α7 deletion may be composed of the same non-α7 components. Alternatively, the presynaptic receptors in α7 antisense-treated cultures may be entirely distinct in subunit composition. Our previous work on MHN channels (*9*) as well as previous studies of heterologous expression of nAChR subunit genes (*2*) would implicate α4 ± α2 and β2 ± β4 subunits in these receptors. This would yield a receptor with high nicotine affinity that is resistant to αBgTx, as is the case after α7 deletion. The antisense mediated deletion of α7 shows that this subunit is a component of the presynaptic nAChR complexes that normally regulate excitatory synaptic transmission in the CNS.

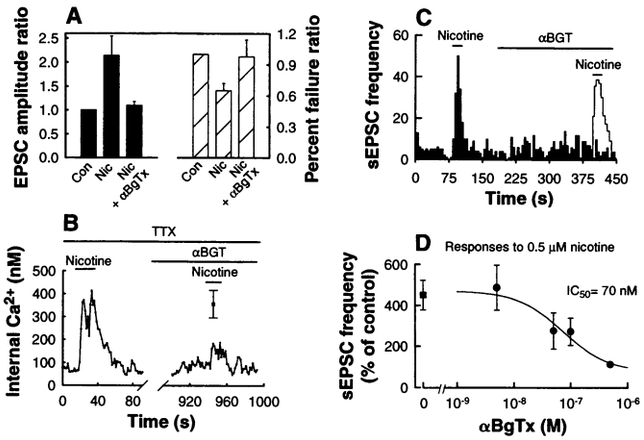

Fig. 4. Inhibition of nicotine-induced presynaptic enhancement by α-bungarotoxin. (**A**) αBgTx effects on nicotine enhancement of evoked EPSCs. Histogram of evoked EPSC amplitude (solid bars), and percent failures (hatched bars) in response to a constant stimulus, under control (con), nicotine (nic; 100 nM, $n = 4$), and nicotine + αBgTx (100 nM, $n = 8$) conditions (MHN-IPN synapses). (**B**) αBgTx effects on nicotine-induced increase in $[Ca^{2+}]_i$. The change in $[Ca^{2+}]_i$ was assayed in VMT explant neurites (as in Fig. 3G) in response to nicotine (10 μM). After a 15 min recovery period, nicotine was applied for a second time, in the presence or absence (isolated data point) of αBgTx (500 nM; 14 min treatment, $n = 3$). (**C**) αBgTx effects on nicotine-induced enhancement of sEPSC frequency. We first determined that the cell was responsive by measuring the effects of nicotine (500 nM) and then, after a 10 min recovery period, nicotine was applied for a second time, in the presence (filled bars) or absence (open bars) of αBgTx (100 nM; ~9 min), $n = 9, 5$ for VMT-LSG and MHN-IPN synapses, respectively. Neither αBgTx or nicotine effected sEPSC amplitude in either preparation. (**D**) αBgTx inhibition of synaptic enhancement is concentration dependent with an IC_{50} ~70 nM (VMT-LSG synapses).

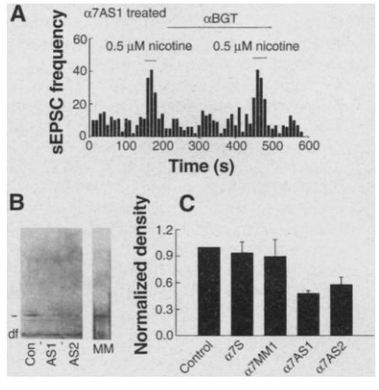

Fig. 5. Effect of antisense oligonucleotide deletion of the α7 subunit. (**A**) Pretreatment of VMT-LSG cultures with antisense oligonucleotides to the α7 subunit mRNA eliminated the αBgTx -sensitivity of nicotine-induced synaptic enhancement (*24, 25*) (αBgTx concentration, 500 nM). (**B**) Immunoblots of total protein from VMT explant cultures probed with an α7 polyclonal antisera (*26*). The line indicates the extent of migration for a 50-kD protein, which is the predicted size of the α7 protein (*21*). Con, denotes untreated control cultures; AS1, AS2, and MM denote α7AS1, α7AS2, and α7MM1, respectively (*24*); df, dye front. (**C**) The amount of α7 protein relative to control was determined by densitometric measurement of autoradiograms. Measurements were normalized to control protein amounts and these values were averaged from three experiments. The α7AS1 and α7AS2 are two antisense oligos spanning the translation start site, α7S is the sense sequence corresponding to α7AS1, and α7MM is the mismatched oligo similar to α7AS1 (*24, 25*).

Conclusions. These findings converge with previous morphological, biochemical, and autoradiographic studies (*27–29*) in support of a simple hypothesis: the predominant, if not exclusive role of CNS nAChRs may be to modify excitability. This idea is based on (i) the sparse experimental support for direct nAChR-mediated synaptic transmission between CNS neurons, (ii) the prominent expression of nicotine and αBgTx binding sites in terminal fields of limbic and cortical areas implicated in cognition and behaviors that are altered by nicotine administration (*27*), and (iii) previous demonstrations that nicotine can stimulate the release of inhibitory transmitters (*28*) as well as modulatory transmitters including norepinephrine and dopamine in numerous synaptosomal studies (*29*). In addition, the localization of nAChRs to presynaptic terminals provides a mechanism whereby the activation of only a few nAChRs could alter excitability. Finally, in view of the potency of nicotine in enhancing glutamatergic synapses and the concentrations of nicotine achieved with smoking, it seems likely that pre- rather than postsynaptic nAChRs mediate the broad psychophysical effects of nicotine in humans.

REFERENCES AND NOTES

1. D. M. Warburton, *Prog. Neuro-Psychopharmacol. Biol. Psychiatry* **16**, 181 (1992); I. P. Stolerman, in *Nicotine Psychopharmacology: Molecular, Cellular, and Behavioural Aspects*, S. Wonnacott, M. A. H. Russell, I. P. Stolerman, Eds. (Oxford University Press, Oxford, 1990), pp. 278–306; E. T. Iwamoto, *J. Pharmacol. Exp. Ther.* **257**, 120 (1991).

2. P. B. Sargent, *Annu. Rev. Neurosci.* **16**, 403 (1993); D. S. McGehee and L. W. Role, *Annu. Rev. Physiol.* **57**, 521 (1995).
3. M. Zhang, Y. T. Wang, D. M. Vyas, R. S. Neuman, D. Bieger, *Exp. Brain Res.* **96**, 83 (1993).
4. F. A. Edwards, A. J. Gibb, D. Colquhoun, *Nature* **359**, 144 (1992).
5. D. A. Brown, R. J. Docherty, J. V. Halliwell, *J. Physiol.* **341**, 655 (1983).
6. N. L. Benowitz, H. Porchet, P. Jacob, in *Nicotine Psychopharmacology: Molecular, Cellular, and Behavioural Aspects*, S. Wonnacott, M. A. H. Russell, I. P. Stolerman, Eds. (Oxford Univ. Press, Oxford, 1990), pp. 112–157.
7. J. R. Wilson, J. C. Mitchell, G. W. Van Hoesen, *J. Comp. Physiol. Psychol.* **78**, 442 (1972); D. Wirtshafter, *Physiol. Behav.* **26**, 985 (1981).
8. E. Wada *et al.*, *J. Comp. Neurol.* **284**, 314 (1989); K. Dineley-Miller and J. Patrick, *Mol. Brain Res.* **16**, 339 (1992).
9. A. B. Brussaard, X. Yang, J. P. Doyle, S. Huck, L. W. Role, *Pfluegers Archiv. Eur. J. Physiol.* **429**, 27 (1994).
10. E. M. Sorenson, D. Parkinson, J. L. Dahl, V. A. Chiappinelli, *J. Comp. Neurol.* **281**, 641 (1989).
11. Embryonic chicken MHN-IPN cocultures were established by plating microexplants of the habenula nucleus (including both the medial and lateral portions) with dispersed IPN neurons. Culture methods were as described (*9, 14*), except that the MHN microexplants were plated 6 to 12 hours before the IPN neurons. Electrophysiology: Cells were visualized on a phase contrast microscope (Zeiss IM 35). Membrane currents were measured by the whole-cell configuration of the patch clamp [O. P. Hamill, A. Marty, E. Neher, B. Sakmann, F. J. Sigworth, *Pflugers Archiv.* **391**, 85 (1981)] with amphoteracin-permeabilized patches [R. Horn and A. Marty, *J. Gen. Physiol.* **92**, 145 (1988); J. Rae, K. Cooper, P. Gates, M. Watsky, *J. Neurosci. Meth.* **37**, 15 (1991)]. The intracellular solution included (in mM) 53 KCl, 75 K_2SO_4, 5 $MgCl_2$, 10 Hepes, and 200 μg/ml amphoteracin, pH = 7.2. The external solution included (in mM) 145 NaCl, 2.5 KCl, 1 $MgCl_2$, 1 $CaCl_2$, and 10 Hepes, pH = 7.4. Voltage clamp recordings were done with a List EPC-7 Patch Clamp amplifier (Medical Systems). In all recordings a holding potential of −80 mV was maintained, unless otherwise noted. Bipolar stimulating electrodes (Frederick Haer) were placed inside the explants, and current injections were applied using a digital pulse generator (World Precision Instruments). Membrane currents were recorded continuously with a video cassette recorder (Sony) through a digital recorder interface (Neurodata Instruments). Evoked EPSCs were triggered and later analyzed with a microcomputer (Gateway 486DX2 50 MHz) equipped with a Labmaster TL-1 A/D interface (Scientific Solutions) and Pclamp software (Axon Instruments). Spontaneous synaptic current data were digitized at 5 kHz and filtered at 1 kHz using an 8-pole Bessel filter (Frequency Devices) and analyzed off-line with custom software written by T. Tsujimoto in C (Borland), and by C. F. Stevens and A. Kyrosis in Axobasic (Axon Instruments). Statistical analyses of sEPSC amplitude data were done using the cumulative distributions to apply the Komolgorov-Smirnov (lilliefors) statistical test [W. Press, B. Flannery, S. Teukolsky, W. P. Vettering, in *Numerical Recipes: The Art of Scientific Computing* (Cambridge University Press, New York, 1986), p. 472]. The percent increase in sEPSC frequency was determined by comparing the average number of events per bin during the control period with the average during the peak of the nicotine response (no less than 3 bins averaged). Biasing of the data by "left censoring" was avoided by setting the bin size to the smallest interval that yielded few or no empty bins.
12. MHN neurons comprise only about 50 percent of the cells in the microexplants. Because they are the only cells in the explanted tissue that express nAChRs (*8, 9*), those synapses that are not altered by nicotine are most likely non–MHN-IPN synapses.
13. VMT-LSG cocultures were prepared as described (*14*). Recording solutions were the same as above with the exception that whole-cell recordings (not permeabilized-patch) were performed in these cells. Intracellular solution included (in mM) 150 KCl, 3 NaCl, 1 $MgCl_2$, 1 EGTA, and 10 Hepes, pH = 7.2. The bath temperature was maintained at 37°C and monitored with a telethermometer.
14. L. W. Role, *Proc. Natl. Acad. Sci. U.S.A.* **85**, 2825 (1988); R. Gardette, M. D. Listerud, A. B. Brussaard, L. W. Role, *Dev. Biol.* **147**, 83 (1991).
15. E. M. Schuman and D. V. Madison, *Annu. Rev. Neurosci.* **17**, 153 (1994); M. S. Fazeli, *Trends Neurosci.* **15**, 115 (1992); S. A. Siegelbaum and E. R. Kandel, *Curr. Opin. Neurobiol.* **1**, 113 (1991).
16. S. Vernino, M. Amador, C. W. Luetje, J. Patrick, J. A. Dani, *Neuron* **8**, 127 (1992); S. Vernino, M. Rogers, K. A. Radcliff, J. A. Dani, *J. Neurosci.* **14**, 5514 (1994); M. M. Rathouz and D. K. Berg, *ibid.*, p. 6935.
17. The data presented in Fig. 3, A and C, address whether postsynaptic increases in $[Ca^{2+}]_i$ are involved in the effect of nicotine on synaptic transmission. Independent assays of changes in $[Ca^{2+}]_i$ under conditions in which the neuron was either depolarized or dialyzed with 10 mM BAPTA supported our contention that these manipulations lead to the predicted changes in intracellular $[Ca^{2+}]$ (Fig. 3, D and E). This experiment does not rule out the possibility that postsynaptic specializations, including structures with a high surface-to-volume ratio, could result in local increases in $[Ca^{2+}]_i$ that would not be effectively buffered by 10 mM BAPTA.
18. Fura-2 imaging of $[Ca^{2+}]_i$ was visualized by means of a Zeiss IM 135-TV microscope equipped with an intensified CCD camera (Hamamatsu) and a Videoprobe imaging system (ETM Systems). Cells were treated with fura 2-AM (10 μM) for 30 min and washed before imaging. Ratios of fluorescent light intensity were calculated and converted to $[Ca^{2+}]_i$ with the formula:

$$[Ca^{2+}]_i = (R - R_{min})(R_{max} - R)^{-1}K_dS_f$$

[G. Grynkiewicz, M. Poenie, R. Y. Tsien, *J. Biol. Chem.* **260**, 3440 (1985)] where R is the fluorescence ratio, R_{max} is the maximum ratio value measured at high $[Ca^{2+}]_i$, R_{min} is the minimum ratio value measured at low $[Ca^{2+}]_i$, K_d is the dissociation constant for Ca^{2+} binding to fura-2, and S_f is a proportionality coefficient. The values for R_{max}, R_{min}, and S_f were determined by in vivo calibration [M. J. S. Heath, T. Lints, C. J. Lee, J. Dodd, *J. Physiol.* **486.1**, 139 (1995); D. A. Williams and F. S. Fay, *Cell Calcium* **11**, 75 (1990)].
19. S. Heinemann *et al.*, *Progr. Brain Res.* **86**, 195 (1990).
20. P. Seguela, J. Wadiche, K. Dineley-Miller, J. A. Dani, J. W. Patrick *J. Neurosci.* **13**, 596 (1993).
21. S. Couturier *et al.*, *Neuron* **5**, 847 (1990); R. Schoepfer, W. G. Conroy, P. Whiting, M. Gore, J. Lindstrom, *ibid.*, p. 35; V. Gerzanich, R. Anand, J. Lindstrom, *Mol. Pharmacol.* **45**, 212 (1994).
22. X. Yang and L. Role, unpublished observation.
23. R. Anand, X. Peng, J. J. Ballesta, J. Lindstrom, *Mol. Pharmacol.* **44**, 1046 (1993); K. T. Keyser *et al.*, *J. Neurosci.* **13**, 442 (1993); R. Anand, X. Peng, J. Lindstrom, *FEBS Lett.* **327**, 241 (1993).
24. Antisense oligonucleotides to the α7 transcription start site (*25*) were stored lyophilized at −20°C. Two antisense oligonucleotide sequences, α7AS1 (G**CAT**CAGCGCCCGGA) and α7AS2 (CAGCCA-CAG**CAT**CAG) (bases complementary to start site in bold) were used with qualitatively similar results. Control oligonucleotides included a sense oligo, α7S complementary to the α7AS1 sequence above, and two mismatch oligos: α7MM1 (GCAACAGAGC-CAGGA) and α7MM2 (CATCCACGGCAACAG), in which the underlined bases are complements to the bases in the same positions in the antisense (Oligos, Etc., Wilsonville, OR). On the day of explant plating, antisense and control oligonucleotides were dissolved in culture media to a concentration of 10 μM. Newly dissected explants were suspended in this solution and added to the culture dishes. Media containing control and antisense oligonucleotides was replenished at 24-hour intervals before recording or collecting for protein measurements. The antisense treatments did not affect neurite outgrowth, synapse formation, synaptic transmission (this study), or the function of K^+ channel and $GABA_A$ receptors (*25*). The specificity of the α7 antisense for α7 per se is underscored by the inactivity of the sense and mismatch oligonucleotides. This, combined with the finding that two different α7 antisense oligos were effective in reducing α7 protein expression, the effects of nicotine, and the sensitivity of these effects to αBgTx, provides evidence that the antisense oligos specifically targeted the α7 mRNA.
25. M. Listerud, A. B. Brussaard, P. Devay, D. R. Colman, L. W. Role, *Science* **254**, 1518 (1991).
26. Protein immunoblot analysis of α7 protein: Culture dishes were washed in phosphate-buffered saline (PBS) and tissue was collected in 1 percent triton-X100 lysis buffer. Each sample was assayed for total protein (BioRad Protein Assay Kit) to enable equivalent loading. The samples were fractionated on a 10% polyacrylamide gel electrophoresis (PAGE) denaturing protein gel and transferred to polyvinylidene fluoride membrane. The α7 protein was assayed with antisera to an α7 fusion protein (1:1000 dilution). The α7 antisera was produced in rabbit (Pocono Rabbit Farm & Laboratory) by injection of an α7-glutathione S-transferase (GST) fusion protein expressed in bacteria. The fusion protein contained part of the intracellular loop of the α7 subunit (amino acids 332 to 387). Immunoglobulins were purified from the serum by the E-Z-Sep purification system (Middlesex Sciences) and depleted with the GST peptide. Antibody binding was visualized with a horseradish peroxidase (HRP)-conjugated antibody to immunoglobulins (1:5000 dilution; Boehringer Mannheim) and enhanced chemiluminescence (ECL, Amersham), per manufacturer's instructions. Densitometric determination of relative protein amounts were measured on a Model 300 Densitometer (Molecular Dynamics). The additional bands visualized on the immunoblot may represent differentially modified protein (α7 has multiple glycosylation sites) or partially degraded α7 protein.
27. P. B. S. Clarke and A. Pert, *Brain Res.* **348**, 355 (1985); G. S. Hamill, P. B. S. Clarke, A. Pert, D. M. Jacobowitz, *J. Comp. Neurol.* **251**, 398 (1986); P. B. S. Clarke, G. S. Hamill, N. S. Nadi, D. M. Jacobowitz, A. Pert, *ibid.*, p. 407.
28. C. Vidal and J.-P. Changeux, *Neuroscience* **29**, 261 (1989); C. Lena, J.-P. Changeux, C. Mulle, *J. Neurosci.* **13**, 2680 (1993); L. L. McMahon, K. W. Yoon, V. A. Chiappinelli, *Neuroscience* **59**, 689 (1994).
29. S. Grady, M. J. Marks, S. Wonnacott, A. C. Collins, *J. Neurochem.* **59**, 848 (1992); H. El-Bizri and P. B. S. Clarke, *Br. J. Pharmacol.* **111**, 414 (1994); Z. J. Yu and L. Wecker, *J. Neurochem.* **63**, 186 (1994); S. Wonnacott, A. Drasdo, E. Sanderson, P. Rowell, *Ciba-Found-Symp.* **152**, 87 (1990).
30. We thank S. Siegelbaum for helpful suggestions for the manuscript, R. Kenter for excellent technical assistance, and Y. H. Kuo for assistance in performing immunoblot analyses of α7 protein. Supported by NIH awards NS22061 to L.W.R. and NS09395 to D.S.M. and by the Council for Tobacco Research and the McKnight Foundation. M.J.S.H. is supported by a Young Investigator Award from the Foundation for Anesthesia Education and Research with a grant from Ohmeda. S.G. is supported by an NIH Medical Scientist Training Program Grant award.

14 March 1995; accepted 8 August 1995